applied sciences

MDPI

Article

High-Precision Productivity Prediction of Fractured Wells in Low-Permeability Reservoirs

Yanjiao Jiang [1,2,*], Yuhan Liu [1,2] and Jian Zhou [1,3,*]

[1] State Key Laboratory of Continental Shale Oil, Northeast Petroleum University, Daqing 163318, China
[2] School of Earth Sciences, Northeast Petroleum University, Daqing 163318, China
[3] School of Physics and Electronic Engineering, Northeast Petroleum University, Daqing 163318, China
* Correspondence: jyjiao0224@163.com (Y.J.); zhouj87@163.com (J.Z.)

Abstract

Long-fractured vertical wells have been widely applied to improve the productivity of low-permeability reservoirs in Area A. However, an efficient and accurate productivity prediction method for the target reservoir has yet to be established. This study aims to clarify the effects of reservoir and fracture parameters on productivity under different formation permeability conditions and to develop a practical productivity prediction method for long-fractured vertical wells. A three-dimensional reservoir numerical simulation model was established to analyze the effects of basic reservoir, well, and fracturing parameters on daily oil production. The results show that daily oil production from the X oil layer increases with formation permeability, effective reservoir thickness, production pressure drawdown, fracture half-length, fracture width, and fracture permeability, but decreases with water saturation, crude-oil viscosity, and skin factor. Numerical simulation further indicates that a fracture half-length of approximately 200 m, fracture permeability of about 300 D, and fracture width of around 6 cm provide favorable productivity responses under the studied conditions, providing a basis for fracturing parameter selection. Based on fractured-well flow theory and triangular fracture morphology, a productivity prediction model was subsequently established. The initial agreement rate between the predicted and well-test productivity values was 81.1%. For layers with discrepancies between the predicted and tested productivity values, numerical simulation was further used to adjust the relevant model parameters, increasing the agreement rate to 91.0%. These results represent a field benchmarking of the consistency between predicted and measured productivity. The proposed method integrates reservoir characterization, numerical simulation, and flow theory, providing an efficient approach for productivity prediction of long-fractured vertical wells in low-permeability reservoirs. The results provide insights into the effects of reservoir and fracture parameters on productivity and a practical reference for fracturing design and reservoir development.

Keywords: low-permeability reservoir; fractured well; reservoir simulation; influencing factors; productivity prediction

Check for updates

Academic Editor: Marco Zucca

Received: 17 August 2026
Revised: 12 October 2026
Accepted: 16 October 2026
Published: 23 October 2026

Copyright: © 2026 by the authors. Licensee MDPI, Basel, Switzerland. This article is an open access article distributed under the terms and conditions of the Creative Commons Attribution (CC BY) license.

1. Introduction

Productivity prediction is a fundamental technique for evaluating reservoir production capacity and has long been an important challenge in oil and gas field development. Reliable productivity prediction provides a scientific basis for reserve evaluation, development planning, production strategy design, and stimulation optimization. Hydraulic

fracturing is one of the primary stimulation techniques for improving the productivity of low-permeability and unconventional reservoirs [1–3]. Therefore, accurately predicting the productivity of fractured wells is particularly important for optimizing fracturing design and reservoir development.

Previous studies have developed several approaches to fractured-well productivity prediction, including statistical regression, theoretical/seepage-flow models, numerical simulation, and machine-learning methods [4–22]. Statistical methods establish empirical relationships between productivity and reservoir or fracture parameters using core, logging, testing, and production data [4–7]. They are relatively convenient for field application but depend strongly on the representativeness and quality of the available data and may have limited applicability outside the calibrated conditions [8,9]. Theoretical methods describe the relationship between fracture geometry, fracture conductivity, reservoir flow, and well productivity based on seepage-flow theory [1,10–12]. These methods have clear physical meanings and are suitable for rapid prediction, but simplifying assumptions regarding fracture geometry and flow conditions may reduce their accuracy in heterogeneous reservoirs [2,4,13]. Numerical simulation can explicitly incorporate reservoir properties, fluid characteristics, well conditions, and fracture parameters, and has therefore been widely used to investigate the productivity response to different fracturing designs [14–16]. However, detailed reservoir modeling and repeated simulations are computationally demanding, which limits their efficiency for rapid field-scale prediction [17]. Machine-learning methods can capture nonlinear relationships and interactions among multiple variables [18–20], but their predictive performance depends on the quantity and quality of training data, and the resulting models may have limited physical interpretability [21–24]. Thus, existing methods involve a trade-off between physical representation, prediction accuracy, and computational efficiency.

Area A of the Daqing Oilfield is located in the western part of the Changyuan area, where the X layer is a key exploration and development target with considerable potential. The reservoirs mainly consist of fine sandstones and siltstones with poor physical properties, belonging to delta front deposits. They represent favorable zones for hydrocarbon migration and accumulation, dominated by lithologic and structural–lithologic reservoirs. In addition, strong reservoir heterogeneity and the complex effects of fracture parameters increase the uncertainty and difficulty of productivity prediction. Therefore, an efficient method that can characterize the effects of reservoir and fracture parameters and provide reliable productivity prediction for fractured wells is needed.

For the target X layer, the key issue is therefore not simply predicting production from existing data, but determining the impact relationship between reservoir/fracture parameters and productivity, and then incorporating this relationship into an efficient prediction method. In particular, the effects of fracture half-length, fracture width, and fracture permeability on productivity need to be evaluated under different permeability reservoir conditions. Meanwhile, a theoretical prediction method should be established while considering the flow characteristics of fractured-well. To address these issues, this study first establishes a three-dimensional numerical reservoir model based on the stratigraphic conditions, petrophysical properties, and fluid characteristics of the study area. Numerical simulations are conducted to identify the key factors controlling productivity and determine favorable fracture parameters. Based on fractured-well seepage-flow theory and triangular fracture morphology, a productivity prediction model is then developed. For layers showing significant deviations between the theoretical prediction and well-test results, numerical simulation is further used to adjust the model parameters and improve the agreement between predicted and measured productivity.

This study provides insights into the effects of reservoir and fracture parameters on productivity by integrating numerical simulation with a physics-based seepage-flow prediction method and establishes a practical evaluation workflow for predicting the productivity of fractured vertical wells in low-permeability reservoirs. The results can support fracture parameter selection and subsequent reservoir development in the study area and offer a useful reference for studies of similar reservoirs.

2. Theory and Methodology

2.1. Numerical Simulation Model

Based on the actual formation conditions, petrophysical properties, and test data of Area A, a vertical-well simulation model was established for the sandstone reservoir in Layer X. In the numerical model, fractures in the vertical well were represented as long, straight, planar fractures symmetrically distributed on both sides of the wellbore. The fracture half-length, width, and permeability were used to characterize the primary geometric and flow properties of the fractures [25]. To simulate the production response of fractured wells, fractures were incorporated into the natural productivity model using local grid refinement, and the corresponding fracture parameters were assigned to the refined grids. Figure 1 shows the top view of the formation model for the fractured vertical well.

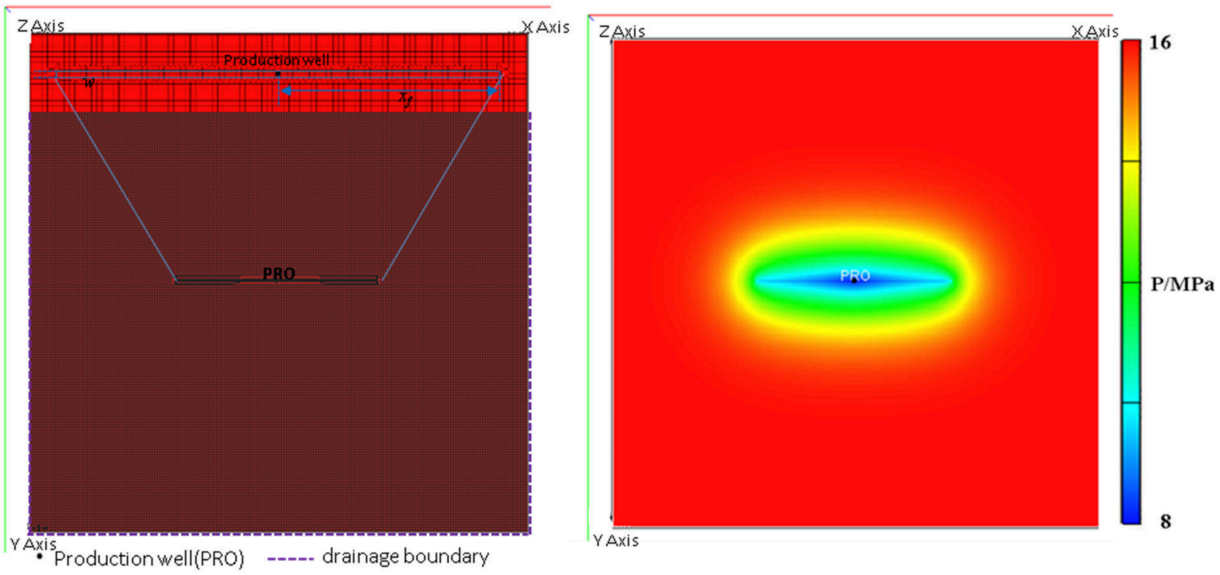


Figure 1. The top view of the fracturing well formation model: (**a**) construction of the fracture through local grid refinement; (**b**) example diagram of formation pressure in the early stage of fracturing well.

The basic model parameters were determined according to the geological and development conditions of the target layer. Table 1 summarizes the basic model parameters. To investigate the effects of the main reservoir and fracture parameters on productivity, eight reservoir parameters and three fracture parameters were selected for sensitivity analysis based on the established numerical simulation model [26]. A one-factor-at-a-time sensitivity analysis was adopted, in which only one parameter was varied in each simulation while all other parameters were maintained at their base-case values. Therefore, interaction effects among different parameters were not considered. For each influencing factor, several parameter values were selected within the actual or experimentally determined range. The resulting daily oil production was recorded for each simulation case, and cross-plots were constructed to characterize the relationship between each parameter and productivity. Considering the petrophysical properties of the target layer, numerical simulations were

conducted under three formation permeability conditions, with permeability values of 1, 10, and 100 mD, to investigate the productivity response under different reservoir permeability conditions. The specific parameter ranges and simulation cases for the individual sensitivity analyses are described in the relevant sections of the Results.

Table 1. Numerical simulation data of formation model.

Parameter	Value	Parameter	Value
Number of grids	100 × 100 × 5	Grid length (m)	10, 10, 1
Top depth (m)	2000	Formation thickness (m)	5
Initial oil saturation (%)	50	Permeability (mD)	1, 10, 100
Oil density (g/cm^3)	0.85	Anisotropic coefficient	1
Oil volume factor	1.1	Water density (g/cm^3)	1.07
Formation pressure (MPa)	20	Oil viscosity (mPa·s)	5
Production pressure drawdown (MPa)	10	Water viscosity (mPa·s)	1.5
Wellbore radius (m)	0.1	Rock compression coefficient (psi-1)	5.8×10^{-6}

2.2. Flow Model

The fracture systems formed in actual low-permeability reservoirs following hydraulic fracturing exhibit significant complexity and heterogeneity. Previous studies have shown that when establishing production prediction models, it is necessary to perform appropriate equivalent modeling of complex fracture networks [27,28]. Considering that the actual fracture width in the study area typically decreases gradually from the vicinity of the wellbore toward the fracture tip, this study represents the fracture system using a triangular geometry to simplify the geometric characteristics while retaining their primary flow-conducting properties. Figure 2 shows a schematic of triangular fracture in a vertically fractured well. By using the average fracture width to characterize the equivalent flow-conducting width of triangular fractures, while maintaining an approximately equivalent effective fracture volume, spatially variable width fractures are converted into equivalent parameters suitable for production calculations. This approach not only preserves the primary influence of fracture widths on flow capacity but is also applicable to production prediction models for long-fractured vertical wells in the study area.

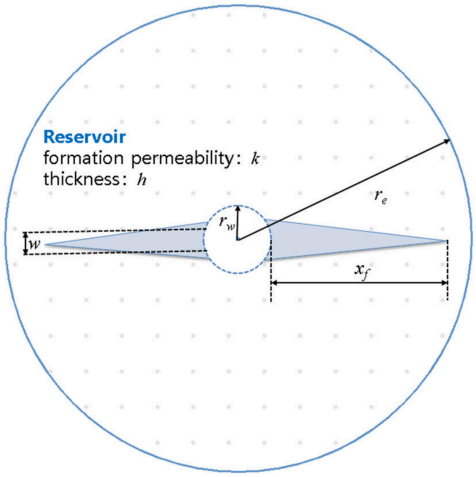


Figure 2. Schematic of a triangular fracture in a vertically fractured well.

Based on a triangular fracture geometry, Raymond and Binder [13] established a productivity calculation formula for vertical fractured wells by applying the equivalent flow resistance method and solving the steady-state flow mathematical model of a composite medium. Using Darcy's law, the production of the X oil layer can be expressed as follows:

$$q = \frac{h(p_e - p_{wf})}{1.842 \times 10^{-3} B\mu \int_{r_w}^{r_e} \frac{1}{rk(r)} dr} \tag{1}$$

where q represents the daily oil production after fracturing, in t·d^{-1}. h represents the effective reservoir thickness, in m. p_{wf} represents bottomhole flow pressure, in MPa. p_e represents external boundary pressure of oil reservoir, in MPa. r_w represents wellbore radius, in m. r_e represents effective drainage radius, in m. $k(r)$ represents the radial permeability distribution at a distance r from the wellbore wall. B represents the crude oil volume factor. μ represents the oil phase viscosity, in mPa·s.

For the near-wellbore formation affected by formation damage, the permeability distribution follows the relationship:

$$\begin{aligned} k(r) &= k_s,\ r_w \le r \le r_s \\ k(r) &= k,\ r_s < r \le r_e \\ k_f(r) &= k_f,\ r_w \le r \le x_f \end{aligned} \tag{2}$$

where r_s represents the radius of the formation damage zone, in m. k_s represents the permeability of the pollution zone, in mD. x_f represents the fracture half-length, in m. k_f represents the fracture permeability, in mD.

Using the integration results from each interval, post-fracturing production is determined:

$$q = \frac{h(p_e - p_{wf})}{1.842 \times 10^{-3} B\mu \frac{k}{k_s} \ln\left(\frac{r_s + \frac{w}{\pi}\left(\frac{k_f}{k} - 1\right)}{r_w + \frac{w}{\pi}\left(\frac{k_f}{k} - 1\right)}\right) + \ln\left(\frac{x_f + \frac{w}{\pi}\left(\frac{k_f}{k} - 1\right)}{r_s + \frac{w}{\pi}\left(\frac{k_f}{k} - 1\right)}\right) + \ln\frac{r_e}{x_f}} \tag{3}$$

where w represents the fracture width, in m. In practical applications, when $k < 1$ mD, $r_s = 0.2$ m; when $1 < k < 10$ mD, $r_s = 0.4$ m; and when $k > 100$ mD, $r_s = 0.8$ m. Based on the degree of formation damage determined from well-test data, k_s is set to $0.1k$.

Based on the empirical correlation between fracture half-length and injected fracturing fluid volume derived from microseismic data interpretation in adjacent regions, the following equation was established:

$$x_f = 0.0619 * Q + 95.14 \tag{4}$$

where Q represents the fracturing fluid volume.

The average fracture width is expressed as follows:

$$w = \frac{M_0}{2hx_f(1 - \phi_f)\rho_b} \tag{5}$$

where M_0 represents the proppant mass, in kg. ρ_b represents the proppant density, in kg·m^{-3}. ϕ_f represents the porosity of the multilayer proppant pack, f.

The fracture permeability is a function of the proppant diameter used during the hydraulic fracturing treatment. According to the Kozeny–Carman equation,

$$k_f = \frac{d_p^2 \phi_f^3}{150\left(1-\phi_f\right)^2} \quad (6)$$

where d_p represents the proppant diameter, in mm. Based on a review of fracturing design data from the study area, when the proppant particle size ranges from 1.68 to 2.38 mm, ϕ_f is approximately 0.32.

The effective drainage radius (re) of the fractured well is expressed as:

$$r_e = \frac{p_e - p_{wf}}{G} \quad (7)$$

where G represents the threshold pressure gradient, in MPa·m^{-1}.

The threshold pressure gradient varies with permeability. For the low-permeability reservoirs in the study area, the following empirical formula is used:

$$G = 0.0682 * K^{-0.9815} \quad (8)$$

3. Results

3.1. Sensitivity Analysis of Basic Parameters

3.1.1. Formation Permeability

Based on core analysis data, the formation permeability range for the simulations was determined, and numerical simulations were conducted using permeability values of 0.1, 0.5, 1, 5, 10, 25, 50, 100, and 200 mD. Figure 3 shows the variation in daily oil production under different permeability conditions. The results indicate that daily oil production generally increases linearly with increasing formation permeability. Increased permeability facilitates more efficient fluid flow through the rock; consequently, this directly translates to higher reservoir production.

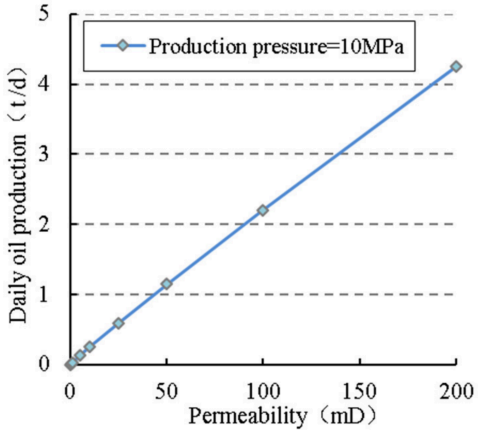


Figure 3. Formation permeability vs. daily oil production.

3.1.2. Formation Effective Thickness

Based on the actual test data, the simulation range of effective reservoir thickness was determined, and numerical simulations were conducted using thickness values of 0.5, 1, 3, 6, 9, 12, 15, and 20 m. Figure 4 shows the relationship between daily oil production and effective reservoir thickness under different formation permeability conditions. The results indicate that daily oil production increases with increasing effective reservoir thickness

under all three permeability conditions, exhibiting a relatively clear linear relationship. This result demonstrates the significant effect of effective reservoir thickness on productivity.

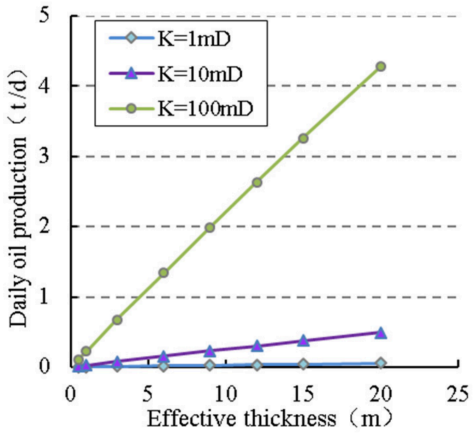


Figure 4. Formation effective thickness vs. daily oil production.

3.1.3. Formation Water Saturation

Numerical simulations were conducted to evaluate the impact of formation water saturation values of 0.2, 0.3, 0.4, 0.5, 0.6, 0.7, and 0.8. Figure 5 shows the relationship between water saturation and daily oil production under different formation permeability conditions. The results indicate that daily oil production decreases with increasing water saturation under all three permeability conditions. The decline is more pronounced in the high-permeability formation, particularly at water saturation below 0.5.

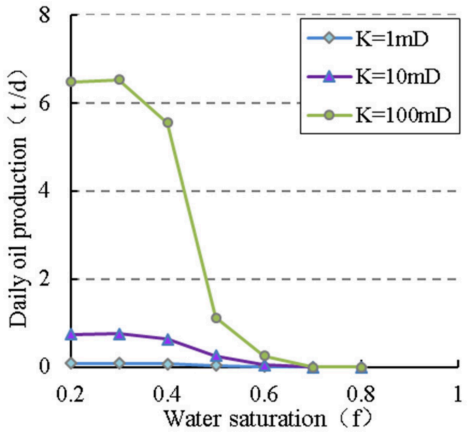


Figure 5. Formation water saturation vs. daily oil production.

3.1.4. Crude Oil Viscosity

Based on well-test data, numerical simulations were conducted for crude oil viscosity values of 1.5, 2, 5, 10, 15, 20, 25, 30, 40, and 50 mPa·s. Figure 6 shows the relationship between crude oil viscosity and daily oil production under different formation permeability conditions. The results indicate that daily oil production decreases with increasing crude oil viscosity under all three permeability conditions. The relationship between crude oil viscosity and daily oil production approximately follows an inverse power-law trend. The decline in daily oil production is more pronounced in high-permeability formation, particularly when crude oil viscosity is below 10 mPa·s. The increase in crude oil viscosity will have a significant impact on oil phase flow, equivalent to an increase in the resistance of the oil phase, thereby reducing daily oil production.

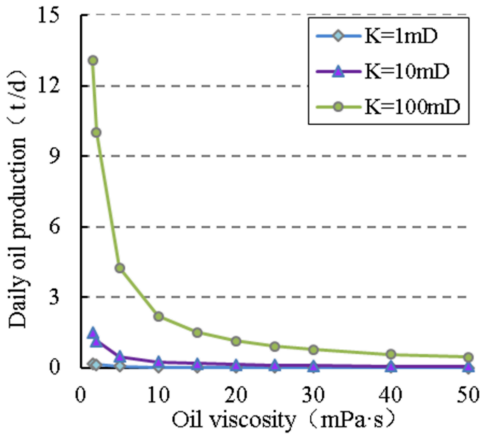


Figure 6. Crude oil viscosity vs. daily oil production.

3.1.5. Crude Oil Volume Coefficient

Numerical simulations were conducted for oil volume coefficient values of 1.00, 1.05, 1.10, 1.15, 1.20, 1.25, 1.30, 1.35, 1.40, and 1.45. Figure 7 shows the relationship between the crude oil volume coefficient and daily oil production under different formation permeability conditions. The results indicate that, under the high-permeability condition (100 mD), daily oil production decreases slightly with increasing crude oil volume coefficient. This effect is less pronounced in low-permeability formations (1 and 10 mD). Compared with crude oil viscosity, the crude oil volume coefficient shows a relatively weaker effect on productivity under the simulated conditions.

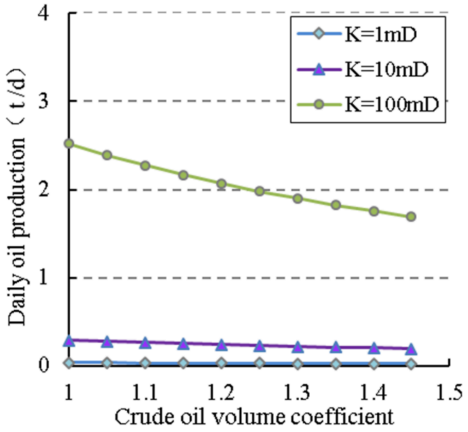


Figure 7. Crude oil volume coefficient vs. daily oil production.

3.1.6. Production Pressure Drawdown

Numerical simulations were conducted for production pressure drawdown values of 1, 3, 6, 9, 12, 15, and 18 MPa. Figure 8 shows the relationship between production pressure drawdown and daily oil production under different formation permeability conditions. The results indicate that daily oil production increases with increasing production pressure drawdown under all three permeability conditions, showing an approximately linear relationship. The similar trends observed under different permeability conditions demonstrate a consistent positive relationship between production pressure drawdown and productivity. Under equivalent pressure changes, formations with higher permeability demonstrate greater increases in daily production. When the permeability of the formation is constant, the greater the production pressure drawdown and the stronger the driving force for fluid flow, resulting in higher oil production.

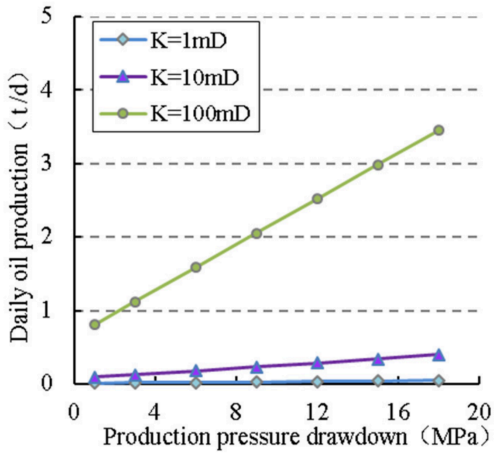


Figure 8. Production pressure drawdown vs. daily oil production.

3.1.7. Skin Factor

Numerical simulations were conducted for skin factor values of −3, −2, −1, 0, 2.5, 5, 7.5, 10, 15, 20, and 25. Figure 9 shows the relationship between skin factor and daily oil production under different formation permeability conditions. The results indicate that daily oil production decreases with increasing skin factor under all three permeability conditions, exhibiting an approximately inverse power-law relationship. The decline in daily oil production is more pronounced in the high-permeability formation. These results demonstrate a clear negative relationship between skin factor and productivity and provide a basis for incorporating skin factor into the subsequent productivity prediction model.

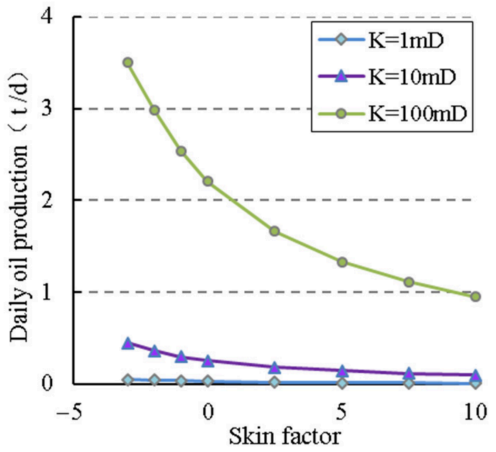


Figure 9. Skin factor vs. daily oil production.

3.1.8. Wellbore Radius

Numerical simulations were conducted for wellbore radius values of 0.075, 0.10, 0.15, 0.20, and 0.25 m. Figure 10 shows the relationship between wellbore radius and daily oil production under different formation permeability conditions. The results indicate that daily oil production increases only slightly with increasing wellbore radius under all three permeability conditions. The effect is particularly limited in the low-permeability formation, where changes in wellbore radius produce little variation in daily oil production. These results demonstrate that wellbore radius has a relatively minor effect on productivity under the simulated conditions and is therefore not considered a primary controlling parameter in the subsequent productivity prediction model.

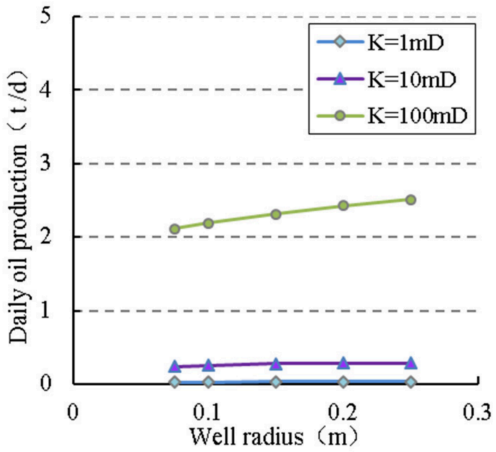


Figure 10. Well radius vs. daily oil production.

3.2. Sensitivity Analysis of Fracture Parameters

To accurately simulate the changes in oil production after reservoir fracturing, local grid refinement is adopted for the fracture regions in the formation model, and corresponding fracture parameters are assigned to carry out detailed simulation research.

3.2.1. Fracture Half-Length

The fracture permeability is set at 300 D, with a fracture width of 5 cm. Simulations were conducted to evaluate the impact of fracture half-lengths of 40, 80, 100, 140, 160, 200, 240, 280, and 300 m on production. Figure 11 shows the simulated daily oil production and cumulative oil production for different fracture half-lengths. The data corresponding to a fracture half-length of 0 m represent the natural production of the well. The simulation results indicate that, under the 100 mD formation permeability condition, increasing fracture half-length produces only a limited increase in oil production. In contrast, for low-permeability formations, both daily and cumulative oil production increase with increasing fracture half-length, indicating a more pronounced productivity response. These results demonstrate that the effect of fracture half-length on productivity is strongly dependent on formation permeability and provide a basis for introducing fracture half-length in the productivity prediction model. However, when the fracture half-length exceeds 200 m, the increase in daily oil production becomes less pronounced. When the fracture half-length increases to a certain level, the production tends to stabilize. Therefore, a fracture half-length of approximately 200 m is considered favorable for production enhancement in low-porosity and low-permeability reservoirs.

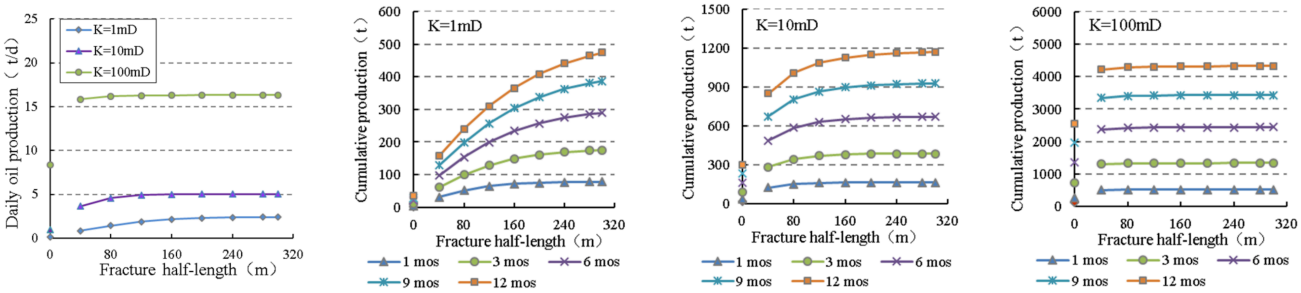


Figure 11. Fracture half-length vs. daily oil production and cumulative oil production.

3.2.2. Fracture Permeability

The fracture half-length and width were fixed at 200 m and 5 cm, respectively. Numerical simulations were conducted for fracture permeability values of 50, 100, 200, 300,

400, 500, and 600 D to evaluate their effects on daily oil production. Figure 12 presents the simulated daily oil production and cumulative oil production for different fracture permeability values. The data corresponding to a fracture permeability of 0 D represent the natural production of the well. Numerical simulation results indicate that as fracture permeability increases, both the daily oil production and cumulative oil production per well significantly improve. For a formation permeability of 1 mD, when the fracture permeability increases from 100 D to 200 D and from 200 D to 300 D, the corresponding increments in cumulative production are 26.3% and 11.1%, respectively. Further increasing the fracture permeability contributes little to additional cumulative oil production. Therefore, for low-porosity and low-permeability formations, a propped fracture permeability of 300 D is considered appropriate.

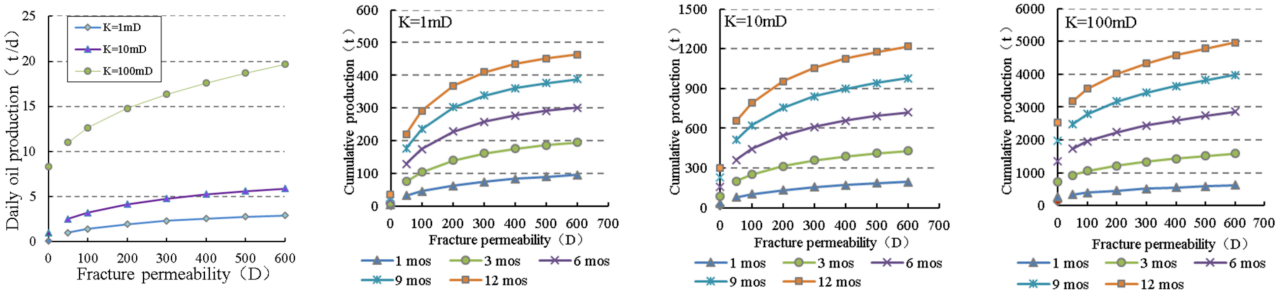


Figure 12. Fracture permeability vs. daily oil production and cumulative oil production.

3.2.3. Fracture Width

The fracture half-length is set at 200 m, with a fracture permeability of 300 D. Simulations were conducted to evaluate the impact of fracture widths of 1, 2, 3, 4,5, 6, 7, and 8 cm on production. Figure 13 presents the simulated daily oil production and cumulative oil production for different fracture widths. The data corresponding to a fracture width of 0 cm represent the natural production of the well. For the formation permeability of 1 mD, cumulative oil production increases by 5.5% when the fracture width reaches 6 cm over a 12-month production period. Further increasing the fracture width results in no significant additional increase in oil production. Therefore, within the investigated parameter range, a fracture width of approximately 6 cm can effectively enhance productivity in low-porosity and low-permeability reservoirs.

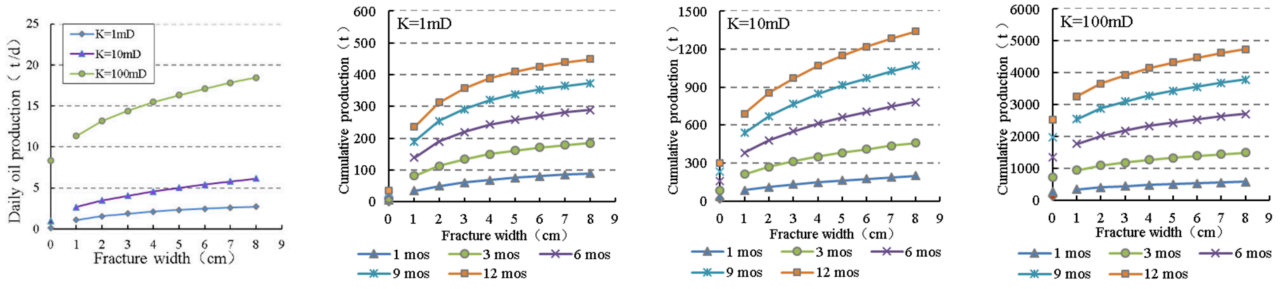


Figure 13. Fracture width vs. daily oil production and cumulative oil production.

4. Case Study

A total of 122 sub-layers from 34 fractured wells in the study area were selected for post-fracturing productivity prediction. The relevant reservoir, fluid, well-test, and proppant parameters were obtained from field measurements and production data. The proposed productivity prediction model based on the flow formulation was applied to

estimate the post-fracturing oil production of these sublayers, and the calculated results were compared with the corresponding well-test results.

The agreement between predicted and measured productivity was assessed using the relative error between the predicted and well-test productivity values. The allowable relative error was determined according to the productivity level of the study area. For example, when the tested productivity is 100 t/d, a relative error of 30% corresponds to an acceptable calculated productivity range of 70–130 t/d. This comparison served as a field-based benchmark for assessing the consistency between predicted and measured productivity, rather than an independent validation of the model. The criteria for relative-error control at different productivity levels are summarized in Table 2.

Table 2. Production accuracy display table based on relative error control.

Test Production Range	Control Relative Error	Example of Production Base	Prediction Lower Limit	Prediction Upper Limit	Explanation
>100	30%	100	70	130	The production within the upper and lower limits is consistent with the production base for testing
50–100	50%	50	25	75	
20–50	70%	20	6	34	
10–20	80%	10	2	18	
1–10	100%	1	0.13	2	
<1	/	1	>0	<1	Matching orders of magnitude while considering production limitations

Based on these criteria, the calculated productivity of the 122 sub-layers was compared with the corresponding tested productivity to evaluate the agreement between the predicted and measured results, as shown in Figure 14. The black lines indicate the relative-error control boundaries. The calculated productivity was consistent with the tested productivity for 99 of the 122 sub-layers, yielding an initial agreement rate of 81.1%.

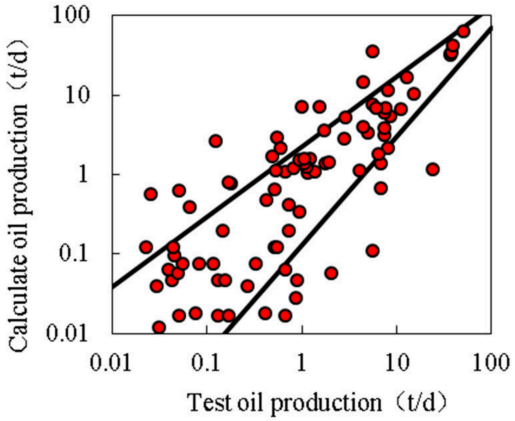


Figure 14. Comparison of test oil production and oil calculated production based on error control.

5. Discussion

The numerical simulation results demonstrate that the productivity of long-fractured vertical wells is jointly controlled by reservoir properties, fluid properties, and fracture parameters, while the impact of these parameters on productivity depend strongly on formation permeability. Daily oil production generally increases with increasing formation permeability, effective reservoir thickness, and production pressure drawdown, whereas increasing water saturation, crude-oil viscosity, and skin factor reduce productivity. These

findings are generally consistent with established seepage-flow theory and previous studies of well productivity, which indicate that reservoir flow capacity and fluid-flow resistance are important controls on well productivity [1,4,8,11,15]. Notably, this study further demonstrates that the productivity response to individual parameters varies under different permeability conditions. For example, the effects of water saturation, crude-oil viscosity, and skin factor on productivity are more pronounced under high-permeability conditions, indicating that formation permeability influences the response of productivity to different controlling factors.

Compared with the basic reservoir parameters, fracture parameters have a more pronounced effect on productivity enhancement in low-permeability formations. Previous studies have shown that increasing fracture half-length, fracture width, and fracture conductivity can enlarge the effective drainage region and reduce flow resistance, thereby improving the productivity of fractured wells [4,10,23]. The numerical simulation results of this study are generally consistent with these findings, but further reveal the dependence of fracture-parameter effects on reservoir permeability. Under the 100 mD condition, further increasing fracture half-length produces only a limited improvement in oil production, whereas under low-permeability conditions, increasing fracture half-length leads to more pronounced increases in both daily and cumulative oil production. Similarly, for the 1 mD formation, cumulative oil production increases by approximately 5.5% over a 12-month production period when the fracture width reaches approximately 6 cm, while further increasing the fracture width produces no significant additional increase in production. These results indicate that a larger fracture size does not necessarily result in a proportionally greater productivity response, because the effectiveness of fracture enlargement is constrained by the flow capacity of the surrounding reservoir. Therefore, fracture parameters should be selected in accordance with reservoir permeability and other reservoir conditions.

For instance, in Layer 46 of the AX9 well, the permeability is only 0.08 mD, and the calculated threshold pressure gradient is 0.81. The measured production pressure drawdown during the well test was 16.98 MPa, resulting in a calculated drainage radius of 82.62 m. The relatively small drainage radius contributed to the deviation between the productivity calculated using the flow formulation and the tested productivity. For layers where the predictions from the production formula method do not agree with the well-test results, examined for reasonableness of calculated reservoir and fluid parameters, the numerical simulation method is applied to adjust and correct the model input parameters so that the simulated output results (such as pressure, production rate, and water cut) match the historical measured data from the oil field. Based on sufficient numerical simulation results and actual fracturing data, the relationship between fracturing-fluid volume and fracture parameters was estimated. This allows for the calibration of key parameters in the production formula. The comparison between the predicted results and the test results after modifying some parameters in 23 layers is shown in Figure 15. The black lines indicate the relative-error control boundaries. According to the standard for matching oil production levels, the coincidence rate reaches 91.0%.

This study still has certain limitations. The sensitivity analysis was conducted using the one-factor-at-a-time method, without explicitly considering the interactions among different parameters. In addition, the fracture geometry was simplified, and some fracture parameters remain difficult to accurately obtain from field data. Therefore, future studies can consider multi-parameter interactions, introduce more complex fracture geometry characterization, and incorporate more field dynamic data to further improve the applicability and predictive capability of the proposed approach in different low-permeability reservoirs.

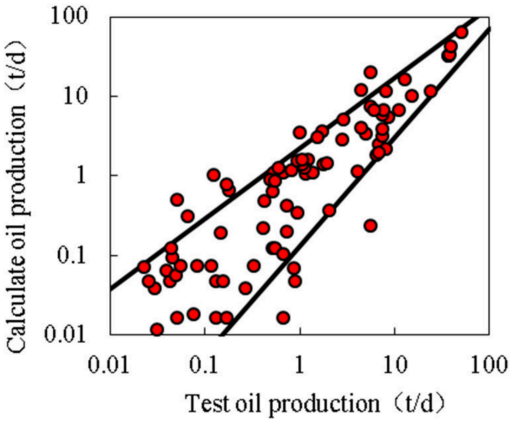


Figure 15. Comparison of test production and the calculated oil production based on the corrected parameters.

6. Conclusions

(1) The numerical simulation results of factors affecting production show that with the increase in formation permeability, effective reservoir thickness, and production pressure drawdown, the daily oil production of the reservoir increases. As the water saturation, crude oil viscosity, and skin factor increase, the daily oil production of the reservoir decreases. These are the main factors affecting reservoir productivity. The influence of water saturation, crude oil viscosity, and skin factor on formations with higher permeability is more significant. The influence of parameters such as wellbore radius and crude oil volume coefficient on reservoir productivity in the study area is not significant.

(2) The numerical simulation results of the fracturing well show that the half-length, width, and permeability of the fractures have a significant effect on increasing the daily and cumulative production of the reservoir. By using reservoir numerical simulation methods, the favorable fracture half-length of the low-permeability reservoir is determined to be about 200 m, the favorable fracture permeability is about 300 D, and the favorable fracture width is about 6 cm, recommended within the investigated parameter range. This provides a basis for selecting fracture parameters for the flow formula method.

(3) For the layers where the predictions from the flow formula method do not match, the numerical simulation method is applied to adjust and revise the model parameters, resulting in an improvement of the coincidence rate of the flow formula method to 91.0%. The combination of numerical simulation and flow formula method can improve the agreement between predicted and measured values of post-fracturing productivity, providing a reliable basis for fracturing productivity prediction in low-permeability reservoirs.

Author Contributions: Conceptualization, Y.J. and J.Z.; methodology, Y.J.; software, Y.J. and Y.L.; formal analysis, Y.J. and Y.L.; investigation, Y.L.; resources, Y.J.; data curation, Y.L.; writing—original draft preparation, Y.J.; writing—review and editing, J.Z.; visualization, Y.L.; supervision, J.Z.; project administration, J.Z.; funding acquisition, Y.J. and J.Z. All authors have read and agreed to the published version of the manuscript.

Funding: This work was supported by Heilongjiang Provincial Natural Science Foundation of China (Grant Number LH2023D011).

Data Availability Statement: The data that support the findings of this study are not publicly available due to confidentiality agreements with the oilfield enterprise. Data may be available from the corresponding author upon reasonable request and with permission from the data owner.

Acknowledgments: The authors thank the reviewers and editors for their valuable comments, which helped improve the manuscript.

Conflicts of Interest: The authors declare no conflict of interest.

References

1. Meng, H.; Eduardo, A.; Ismail, M.B.; Joe, M.M. Production systems analysis of vertically fractured wells. In *SPE Unconventional Gas Recovery Symposium, Pittsburgh, Pennsylvania, May 1982*; SPE-10842; Society of Petroleum Engineers: Houston, TX, USA, 1982.
2. Zou, C.; Zhai, G.; Zhang, G.-Y.; Wang, H.-J.; Zhang, G.-S.; Li, J.-Z.; Wang, Z.-M.; Wen, Z.-X.; Ma, F.; Liang, Y.-B.; et al. Formation, distribution, potential and prediction of global conventional and unconventional hydrocarbon resources. *Pet. Explor. Dev.* **2015**, *42*, 13–25. [CrossRef]
3. Ricardo, C.B.; Sergiy, M.; Hosur, R.L. The challenge to integrate sedimentology and well completion to predict production performance in an unconventional reservoir. In *Proceedings of the Abu Dhabi International Petroleum Exhibition and Conference (ADIPEC), Abu Dhabi, United Arab Emirates, 2–5 October 2023*; SPE-216157-MS; Society of Petroleum Engineers: Houston, TX, USA, 2023; pp. 1–13. [CrossRef]
4. Agarwal, R.G.; Carter, R.D.; Pollock, C.B. Evaluation and performance prediction of low-permeability gas wells stimulated by massive hydraulic fracturing. *J. Pet. Technol.* **1979**, *31*, 362–372. [CrossRef]
5. Poe, B.D. Production performance evaluation of hydraulically fractured wells. In *Proceedings of the SPE/CERI Gas Technology Symposium, Calgary, AB, Canada, 3–5 April 2000*; SPE59758; Society of Petroleum Engineers: Houston, TX, USA, 2000.
6. Liu, Y.; Sun, J.; Yan, C.; Wang, D.; Song, K.; Song, Q. A machine learning-based production prediction method for multi-type fracturing in waterflood reservoirs. In *Proceedings of the SPE Annual Technical Conference and Exhibition, Houston, TX, USA, 20–22 October 2025*; SPE-227919-MS; Society of Petroleum Engineers: Houston, TX, USA, 2025; pp. 1–18. [CrossRef]
7. Chengl, M.L.; Leal, M.A.; Mcnaughton, D. Productivity prediction from well logs in variable grain size reservoirs cretaceous qishn formation, republic of Yemen. *Log Anal.* **1999**, *40*, 24–32.
8. Guan, Y.; Niu, Y.; Han, D.; Zhou, X.; Li, K. Prediction of production in oil reservoirs by considering change in number of production wells. In *Proceedings of the SPE Eastern Regional/AAPG Eastern Section Joint Meeting, Pittsburgh, PA, USA, 11–15 October 2008*; SPE-117149; Society of Petroleum Engineers: Houston, TX, USA, 2008; pp. 1–9.
9. Alali, A.Z.; Tech, T.; Sheng, J.J.; Soliman, M.Y.; Watson, M.C.; Tech, T. Methodology of well productivity prediction from analyzing formation tester probe transient pressure Data in a multilayer reservoir using a new spherical drawdown analysis method. In *Proceedings of the SPE Annual Technical Conference and Exhibition, Amsterdam, The Netherlands, 27–29 October 2014*; SPE-170907-MS; Society of Petroleum Engineers: Houston, TX, USA, 2014; pp. 1–19.
10. Prats, M. Effect of vertical fractures on reservoir behavoir–results on oil and gas flow. *J. Pet. Technol.* **1963**, *15*, 1119–1126. [CrossRef]
11. Yu, S.; Miocevic, D.J.; Canada, C. An improved method to obtain reliable production and EUR prediction for wells with short production history in tight/shale reservoirs. In *Proceedings of the SPE/AAPG/SEG Unconventional Resources Technology Conference, Denver, CO, USA, 12–14 August 2013*; SPE-168684; Society of Petroleum Engineers: Houston, TX, USA, 2013.
12. Pan, B.; Fang, C.; Guo, Y.; Zhang, L.; Lei, J.; Fan, Y. Logging evaluation and productivity prediction of Sulige tight sandstone reservoirs based on petrophysics transformation models. *Chin. J. Geophys.* **2018**, *61*, 5115–5123.
13. Silva, L.C.F.; Portella, R.C.M.; Emerick, A.A.; Ebecken, N.F.F.; Federal, U.; De Janeiro, R. Predictive data-mining technologies for oil-production prediction in petroleum reservoir. In *Proceedings of the Latin American & Caribbean Petroleum Engineering Conference, Buenos Aires, Argentina, 15–17 April 2007*; SPE-107371; Society of Petroleum Engineers: Houston, TX, USA, 2007; pp. 1–5.
14. Kaul, S.P.; Texas, A.; Vaz, R.F.; Gildin, E.; Texas, A. Single block productivity approach–how it identifies and isolates multiple fracture network variants and helps improve history matching and prediction in unconventional reservoirs using reservoir simulator. In *Proceedings of the SPE Reservoir Simulation Conference, Galveston, TX, USA, 10–11 April 2019*; SPE-193900-MS; Society of Petroleum Engineers: Houston, TX, USA, 2019; pp. 1–25.
15. Zhang, S.; Guo, K.; Gao, X.; Yang, H.; Zhang, J.; Han, X. Productivity prediction model of perforated horizontal well based on permeability calculation in near-well high permeability reservoir area. *Energy Eng.* **2024**, *121*, 59–75. [CrossRef]
16. Zhang, Z.; Liao, J.; Li, Z.; Zheng, X.; Di, H.; Yu, P. Fast prediction of productivity level of low permeability reservoirs based on multilayer perceptron–A case study of Chang 3, 4+5 reservoirs of Baibao, Nanliang areas in Ordos basin. *Prog. Geophys.* **2019**, *34*, 1962–1970.
17. Tian, K.; Kang, Z.; Kang, Z. A productivity prediction method of fracture-vuggy reservoirs based on the PSO-BP neural network. *Energies* **2024**, *17*, 3482. [CrossRef]
18. Wang, F.; Cheng, Q.; Ren, L.; Han, L. Well logging capacity evaluation method for tight sandstone gas reservoirs based on SSA-RF modeling. *Nat. Gas Geosci.* **2025**, *36*, 2193–2203.
19. Li, C.; Li, C.; Hou, Y.; Shi, Y.; Wang, C.; Hu, F.; Liu, M. Well logging evaluation of Triassic Chang 7 Member tight reservoirs, Yanchang Formation, Ordos Basin, NW China. *Pet. Explor. Dev.* **2015**, *42*, 608–614. [CrossRef]

20. Gao, Q.; Shang, Y.; Wang, J.; Gao, K.; Ma, J.; Zhang, Z.; Zhang, G. New method for productivity prediction of paleogene middle-deep sandstone reservoir in Bohai Sea area. *Prog. Geophys. Chin.* **2024**, *39*, 1–13.
21. Raymond, L.R.; Binder, G.G. Productivity of wells in vertically fractured, damaged formations. *J. Pet. Technol.* **1967**, *19*, 120–130. [CrossRef]
22. Daungkaew, S.; Claverie, M.; Cheong, B.; Hansen, S.; Leech, R.; Azam, M.N.H.M.; Malim, E.; Lasman, M.R.; Witjaksana, R. Forecasting the productivity of thinly laminated sands with a single well predictive model. In *Proceedings of the SPE Asia Pacific Oil and Gas Conference and Exhibition, Perth, Australia, 20–22 October 2008*; SPE-116370; Society of Petroleum Engineers: Houston, TX, USA, 2008; pp. 1–9.
23. Tong, S.; Wang, F.; Gao, H.; Zhu, W. A machine learning-based method for analyzing factors influencing production capacity and production forecasting in fractured tight oil reservoirs. *Int. J. Hydrogen Energy* **2024**, *70*, 136–145. [CrossRef]
24. Tan, C.; Ma, N.; Su, C. Model and method for oil and gas productivity prediction of reservoir. *J. Earth Sci. Environ. Chin.* **2004**, *26*, 2–6.
25. Jiang, Y.; Sun, J.; Gao, J.; Zhang, P.; Cui, J. A simulation of mud invasion and characteristics of array laterolog responses in a low-permeability gas reservoir: A case study. *J. Geophys. Eng.* **2017**, *14*, 456–465. [CrossRef]
26. Jiang, Y.; Zhou, J.; Zhang, J.; Guo, Z. Trajectory optimization of ultra-short sidetrack horizontal wells in marginal reservoirs. *Front. Earth Sci.* **2025**, *13*, 1533309. [CrossRef]
27. Mahmoodi, S.; Abbasi, M.; Sharifi, M. New fluid flow model for hydraulic fractured wells with non-uniform fracture geometry and permeability. *J. Nat. Gas Sci. Eng.* **2019**, *68*, 102914. [CrossRef]
28. Jiang, L.; Liu, J.; Liu, T.; Yang, D. A semianalytical model for transient pressure analysis of a horizontal well with non-uniform fracture geometry and shape-dependent conductivity in tight formations. *J. Pet. Sci. Eng.* **2020**, *195*, 107860. [CrossRef]

Disclaimer/Publisher's Note: The statements, opinions and data contained in all publications are solely those of the individual author(s) and contributor(s) and not of MDPI and/or the editor(s). MDPI and/or the editor(s) disclaim responsibility for any injury to people or property resulting from any ideas, methods, instructions or products referred to in the content.